NUCLEAR MAGNETIC RESONANCE STUDIES OF CATION TRANSPORT ACROSS VESICLE BILAYER MEMBRANES

DAVID Z. TING, PATRICK S. HAGAN, AND SUNNEY I. CHAN, *Arthur Amos Noyes Laboratory of Chemical Physics, California Institute of Technology, Pasadena, California 91125*

JIMMIE D. DOLL AND CHARLES S. SPRINGER, JR., *Department of Chemistry, State University of New York at Stony Brook, Stony Brook, New York 11794*

ABSTRACT We analyze an increasingly popular NMR method analogous to the black lipid membrane (BLM) isotopic tracer experiment for the study of mediated cation transport but involving the preparation of vesicles with an environment asymmetric in that paramagnetic metal ions are present only outside the vesicles. This asymmetry is manifest in the NMR spectrum as two distinct resonances for magnetic nuclei in outside and inside lipid headgroups. As mediated transport begins and the paramagenetic metal ions enter the vesicles, the inner headgroup resonance line shifts and changes shape with a time course containing much information on the actual ion transport mechanism. Processes by which the ions enter the vesicles one or a few at a time (such as via a diffusive carrier) are easily distinguishable from those by which the ions enter in large bursts (such as by pore activation). The limiting case where intervesicular mediator exchange is slow relative to cation transport (the situation for integral membrane proteins) is treated analytically. Computer simulated curves indicate conditions necessary for certain changes in the line shape which are analogous to the "current jumps" observed in BLM conductance studies. The theory derived allows estimates of the average number of ions entering in the first few bursts, how often the bursts occur, and how they depend on the concentration of the mediating species in the vesicular membrane. Preliminary experimental spectra illustrating some of the various possible line shape behaviors are presented.

INTRODUCTION

The mediated transport of cations across biological membranes is a key feature of many physiological phenomena. An understanding of the various mechanisms of cation transport, on the molecular level, seems most likely to come from the study of model membrane systems. The vast majority of model membrane studies have employed black lipid membrane (BLM) preparations; these have yielded a number of fascinating results (Stevens and Tsien, 1979; McLaughlin and Eisenberg, 1975; Hladky et al., 1974). Perhaps the major advantage of this model system is its amenability to electrical measurements and continuous flow tracer experiments.

However, the BLM model does have some serious drawbacks. One is the apparent difficulty of incorporation of membrane protein mediators (probably the kind of ultimate interest) (Montal, 1976; Shamoo and Goldstein, 1977; Korenbrot, 1977). A second problem is the heterogeneity of the BLM. One of the desired characteristics of a model system is that it be a

simple, homogeneous prototype of the more complicated natural system. This is not true of the BLM, where there is more than one kind of membrane region or "phase" separating the two aqueous phases (White, 1977): "annular" solvent-double lipid monolayer phase, a solvent saturated-lipid bilayer phase, and possibly a "microlens" phase. These phases are apparently unavoidable (Waldbillig and Szabo, 1979; White et al., 1978). The mechanisms and rates of transport through these different membrane phases may differ, at least with certain types of mediated transport. If so, the measured net flux is the sum of the various processes, weighted according to their efficiencies.

Single bilayer vesicles prepared either by ultrasonic irradiation or by carrier dilution do not have either of the above two drawbacks (Montal, 1976; Shamoo and Goldstein, 1977; Barenholz et al., 1977). Reconstitutions of active membrane proteins in vesicles have been successfully accomplished. The generally small size of vesicles poses disadvantages, however. The smallest ones (made by ultrasonic irradiation) have a very small average radius of curvature (~110 Å) and this causes significant differences in packing of the lipids in the inner and outer monolayers (Scott and Cherng, 1978; Chrzeszczyk et al., 1977; Sheetz and Chan, 1972). The transport properties of such bilayers might be different from those of the more planar membranes found in biological cells, although their validity as models for the highly curved regions of natural membranes should not be discounted. A more serious disadvantage, however, has to do with the small inner aqueous cavity (average radius $\simeq$ 75 Å, in the smallest ones). It is seemingly too small to be impaled with even a microelectrode or to allow continuous tracer studies. Thus, the two most productive kinds of BLM experiments seem to be precluded in vesicle studies.

However, single bilayer vesicle preparations are well suited for spectroscopic studies and the NMR method we discuss is completely analogous to the isotopic tracer diffusion technique. In the course of our analysis, we will show that the rather small inner aqueous regions of the smaller vesicles can be exploited to considerable advantage.

NMR SPECTRUM OF SINGLE BILAYER VESICLES IN THE PRESENCE OF PARAMAGNETIC LANTHANIDE IONS

Since the first report by Bystrov and co-workers (Bergelson et al., 1970), there have been many studies describing and exploiting the effect of paramagnetic lanthanide ions on the ^{1}H, ^{31}P, or ^{13}C resonances of vesicle phospholipid molecules (for summaries, see Chrzeszczyk et al., 1976; Hutton et al., 1977; and Bergelson, 1977). When paramagnetic lanthanides are introduced, only into the intervesicular aqueous phase of a vesicle suspension prepared by sonication in the presence of a diamagnetic lanthanide ion, Ln, the situation can be depicted as in Fig. 1, where Ln*, the tracer, is a paramagnetic lanthanide ion as closely isomorphic with Ln as possible. Fig. 1 indicates a system where the concentrations are adjusted such that $[Ln]_{out} + [Ln^*]_{out} = [Ln]_{in}$ so as to avoid the development of diffusion potentials. A comparison of the NMR spectrum of this system with the analogous one containing no ions, or only the diamagnetic ions, shows that there is no effect on the chemical shifts of the hydrocarbon chain resonances. The headgroup resonances, in contrast, are always split into doublets; one component of each doublet is smaller in area and retains the chemical shift exhibited in the absence of the Ln* ion. The larger component of each doublet undergoes a hyperfine shift, the sign and magnitude of which depends upon the Ln* ion chosen. The shifted component is assigned to headgroups of the phospholipid molecules on the outer

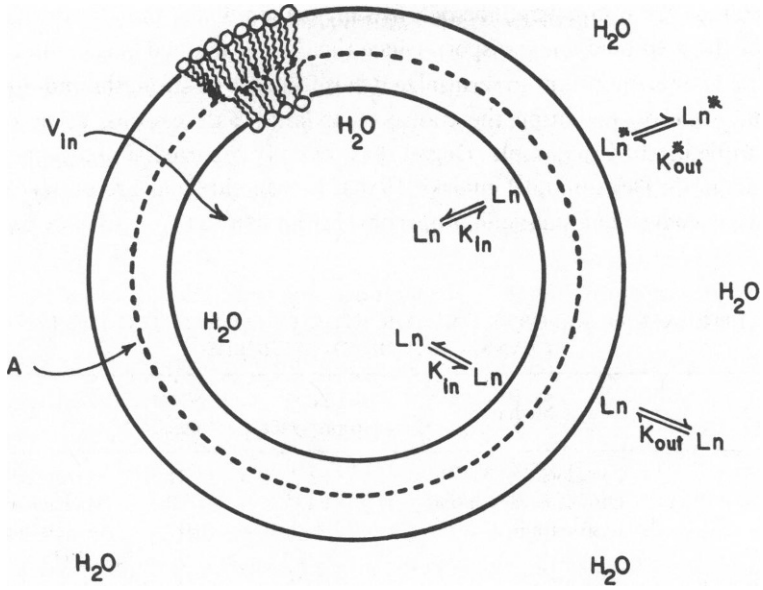

FIGURE 1

surfaces of the vesicles where they are available for interaction with the Ln* ion. The remaining smaller component is assigned to the headgroups on the inner surfaces and the fact that it remains unshifted demonstrates that the metal ions do not permeate into the inner vesicular spaces. Indeed, studies have shown that, depending upon the exact nature of the phospholipid molecules, the thermal history of the sample, and of course the presence or absence of cation transporting mediators, some vesicles can remain impermeable to the lanthanide ions for periods of at least days.

The magnitude of the hyperfine shift of the outer headgroup resonance increases continuously with Ln* ion concentration demonstrating that the kinetics of the ion/surface binding equilibria are rapid on the NMR time scale. Thus, the observed chemical shift is the weighted average over those phospholipid molecules in the outer monolayer which are and are not interacting with the Ln* ion. The quantitative details of the binding of lanthanide ions to phospholipid membrane surfaces (K_{out} and K_{in} in Fig. 1) are complicated by electrostatic factors and probable allosteric effects (Chrzeszczyk, 1978)[1]. However, we can note qualitatively that the binding is strong (stronger than that of divalent metal cations) and, as expected, the interactions of the smaller, more acidic lanthanide ions are somewhat greater than those of the larger members of the period. This is an example of why it is important to have the Ln/Ln*·ion pair as isomorphous as possible. Preferred pairs are La^{+3}/Pr^{+3} and Lu^{+3}/Yb^{+3}. We will discuss further aspects of the lanthanide ion/vesicle binding equilibria below.

The essence of this NMR method of studying metal ion transport is the following. When some process of mediated ion transport is caused to become operative in a vesicle preparation where Ln* ions are present only on the outside, the two components of the headgroups

[1]Chrzeszczyk, Wishnia, and Springer. Manuscript submitted for publication.

resonance begin to come together. The detailed manner in which they do this can reveal the mechanism of the mediated ion transport. Since this NMR method is becoming increasingly popular (Table I), it is important to scrutinize it carefully for its strengths and limitations. If a process is incapable of mediating the transport of lanthanide cations, other paramagnetic metal ions can be used (for example, Degani has recently reported similar experiments with Mn^{+2}; Degani, 1978; Degani and Lenkiski, 1980). Lanthanide ions are preferred because of their particularly convenient magnetic properties. [With Mn^{+2}, $(\nu_0^s - \nu_0^f) = 0$; Eq. 14].

TABLE I
LITERATURE REPORTS ON NMR STUDIES OF LANTHANIDE ION TRANSLOCATION IN VESICLES

Lipid	Mediator	Ln^{+3} transported	NMR nucleus	Reference
Egg lecithin (EL)	Lassalocid A (X-537 A)	Pr^{+3}	^{1}H	Fernandez et al., 1973
EL	Ultrasonic irradiation	Eu^{+3}	^{31}P	Michaelson et al., 1973
EL	Lysolecithin	Pr^{+3}	^{1}H	Bergelson and Bystrov, 1975
Dipalmitoyl-lecithin (DPL)	Alamethicin	Eu^{+3}	^{1}H	Lau and Chan, 1975
DPL	X-537 A, and efrapeptin (calcimycin, A-23187)	Pr^{+3}	^{1}H	Hunt, 1975
DPL	Alamethicin	Eu^{+3}	^{1}H	Lau and Chan, 1976
DPL, and distearoyl-lecithin (DSL)	Ultrasonic irradiation	Eu^{+3}	^{1}H	Lawaczeck et al., 1976
DPL	Ultrasonic irradiation	Pr^{+3}	^{31}P	Chrzeszczyk et al., 1976
EL	Phytanic acid α-tocopherol (vitamin E), and phytol	Pr^{+3}	^{31}P	Cushley and Forrest, 1977
DPL and dimyristoyl-lecithin (DML)	Lysolecithin	Eu^{+3}	^{1}H	Lee and Chan, 1977
DSL, DPL, DML, and dilauroyl-lecithin (DLL)	Thermal	Eu^{+3} and Nd^{+3}	^{1}H	Lawaczeck et al., 1977
EL	Rhodopsin	Eu^{+3}	^{1}H	O'Brien et al., 1977
DPL	Thermal w. cholesterol, and thermal w. hexadecane	Pr^{+3}	^{1}H	Hunt and Tipping, 1978
El, sterol, and dicetylphosphate (DCP)	Nystatin, Triton X-100	Pr^{+3}	^{31}P	Pierce et al., 1978
DPL	A-23187	Pr^{+3}	^{1}H	Hunt et al., 1978
Dioleoyllecithin (DOL)	Glycophorin	Dy^{+3}	^{13}C	Gerritsen et al., 1979
DPL	Cholate, glycocholate, deoxycholate chenodeoxycholate, and cholesterol/chenodeoxycholate	Pr^{+3}	^{1}H	Hunt and Jawaharlal, 1980
DPL	Triton X-100, taurocholate, thermal w. Triton X-100, and thermal	Pr^{+3}	^{1}H	Hunt, 1980

THE TIME-COURSE OF THE OUTER HEADGROUP RESONANCE

The magnitude of the hyperfine shift of the outer resonance depends upon the concentrations of the paramagnetic shift reagent, the lecithin vesicles, and the concentrations of other competitive species. The shape of the curve expressing this dependence (the NMR binding isotherm) depends in turn upon the affinity constant, the limiting hyperfine shift and the limiting stoichiometry (Chrzeszczyk, 1978).[1] For the remainder of this discussion, we shall assume that we are dealing with a system constrained to be on the initial linear region of the NMR binding isotherm (i.e., reasonably far from binding saturation). Thus, for a constant concentration of vesicles, the shift of the outer headgroup resonance is linearly related to the concentration of the paramagnetic lanthanide ion in the external aqueous phase.

Let us say that, before the transport process becomes operative (i.e., when $t = 0$), the outer headgroup resonance is shifted $\Delta_t = \Delta_0$ ppm from its position in the absence of the shift reagent; generally about the same as the position of the inner headgroup resonance. (Under high resolution the inner and outer ^1H and ^{31}P headgroup resonances of the smaller vesicles can be observed to have small (compared to Δ_0) differences in chemical shifts because of differences of headgroup packing (Sheetz and Chan, 1972; Hutton et al., 1977). After the transport process has started, the magnitude of Δ_t will decrease with time and will asymptotically approach its equilibrium value, Δ_∞ (Lawaczeck et al., 1977, Chrzeszczyk et al., 1976). (The quantities Δ_0 and Δ_∞ are depicted in Fig. 2.) The concentration of Ln* ions in the external aqueous solution is being decreased as these ions are transported into the intravesicular compartments of the vesicles. Since the lipid molecules on the outside vesicle surfaces all sample the same external aqueous phase and thus are exposed to the same Ln* ion concentration, the outside headgroup resonance always gives rise to a symmetrical, homogeneous peak. We are assuming that the vesicle size distribution is narrow enough so as not to give rise to any inhomogeneous broadening. Experimental methods for achieving this have been reviewed (Szoka and Papahadjopoulos, 1980). When the transport process is well along to completion, the inside headgroup resonance may begin to overlap the outside headgroup resonance (Chrzeszczyk et al., 1976, *vide infra*) and thus the observed resonance may not appear symmetrical. However, the outside component will always make a symmetrical contribution.

As long as the system is on the linear portion of the NMR binding isotherm, the product of $1 - (\Delta_\infty/\Delta_0)$ and the stoichiometric ratio of Ln* ions to vesicles gives the average number of Ln* ions which have entered a vesicle at equilibrium $\langle Z_{eq} \rangle$. We can easily ascertain the probable limits of $1 - (\Delta_\infty/\Delta_0)$. If the affinity constant were vanishingly small, such that exceedingly few of the ions were bound, $1 - (\Delta_\infty/\Delta_0)$ would be equal to the ratio of the inner vesicular cavity volume to the total aqueous volume (0.01–0.03, in typical experiments; Chrzeszczyk et al., 1977). (In addition, there would probably be no linear region of the binding isotherm.) If the affinity constant were extremely large, such that essentially all of the ions were bound, $1 - (\Delta_\infty/\Delta_0)$ would be equal to the ratio of the inner surface area to the total surface area (~0.33, for typical preparations of small vesicles; Hutton et al., 1977). This latter

[1]Chrzeszczyk, Wishnia, and Springer. Manuscript submitted for publication.

assumes, of course, that any differences in the affinity constants and limiting stoichiometries between the inside and outside surfaces, due to packing differences, are small compared to their magnitudes. (We have, however, recently obtained preliminary data which indicate that K_{in} is noticeably greater than K_{out}; Chrzeszczyk, 1978.)[1] Experimentally, values of $1 - (\Delta_\infty/\Delta_0)$ have been observed to fall within these extremes: 0.10 (Lee and Chan, unpublished results), 0.13 (Chrzeszczyk, 1978), 0.18 (Chrzeszczyk et al., 1976), 0.25 (Springer and Chan, unpublished results). Therefore the magnitude of the affinity constant is such that this factor is sensitive to the values of the aqueous volume and the lipid surface area (as well as the nature of the lipid, the metal ion and other competitive species present). Fortunately, the factor can always be determined experimentally, at the finish of each transport experiment, and can be used in the subsequent interpretation (*vide infra*). This factor is also useful in setting up the experiment so that the two solutions on either side of the vesicle membrane remain isotonic during the entire course of the transport process. If the activity of a mediator is pH sensitive, pH gradients across the membrane can also be avoided by sufficient buffering.

An analysis of the exponential time course of the outside headgroup resonance, as it proceeds from Δ_0 to Δ_∞ should be useful in the determination of the rate and activation parameters of the transport process. As far as mechanistic information is concerned, however, the spectral behavior of the inner headgroup resonance is more revealing and hence of more interest. It is possible to conduct these experiments in such a way that the inner resonances are observed free of overlap with the outer resonances (Hunt, 1975; Pierce et al., 1978; Hunt and Tipping, 1978; Hunt, 1980).

THE TIME-COURSE OF THE INNER HEADGROUP RESONANCE

Qualitatively, the time courses of inner headgroup resonances, during transport, have been found to exhibit at least three intrinsically different types of behavior. We show examples from our laboratories.

The "All or Nothing" Process

Fig. 2 depicts the ^{31}P-NMR spectrum of small dipalmitoyl-lecithin (DPL) vesicles as the transport of Pr^{+3} ions from outside to inside is mediated by ultrasonic irradiation. These data are taken from the work of Chrzeszczyk (Chrzeszczyk et al., 1976; Chrzeszczyk, 1978).

Before the transport process begins, the outer DPL resonance is downfield relative to the inner phosphate resonance ($\Delta_0 = -10.5$ ppm). As resonication begins, the outer DPL resonance is seen to shift back upfield exponentially with time ($\Delta_{60} \simeq \Delta_\infty = -9.1$ ppm).

The inner DPL resonance, however, exhibits an extremely interesting behavior. As the elapsed resonication time increases, the intensity of this resonance becomes smaller in relation to the outer DPL resonance but its chemical shift and linewidth remain unchanged. A new peak is seen to grow in downfield of the outer DPL resonance with a hyperfine shift of $\simeq 11.2$ ppm, measured from the position of the orignal inner DPL peak. This new peak can be assigned as the inner DPL resonance of vesicles which have obtained their equilibrium charge of inner Pr^{+3} ions which, in this case, is ~56 on the average (Chrzeszczyk, 1978). (Two ^{31}P-DPL resonances are observed if the vesicles are initially formed in the presence of Pr^{+3}

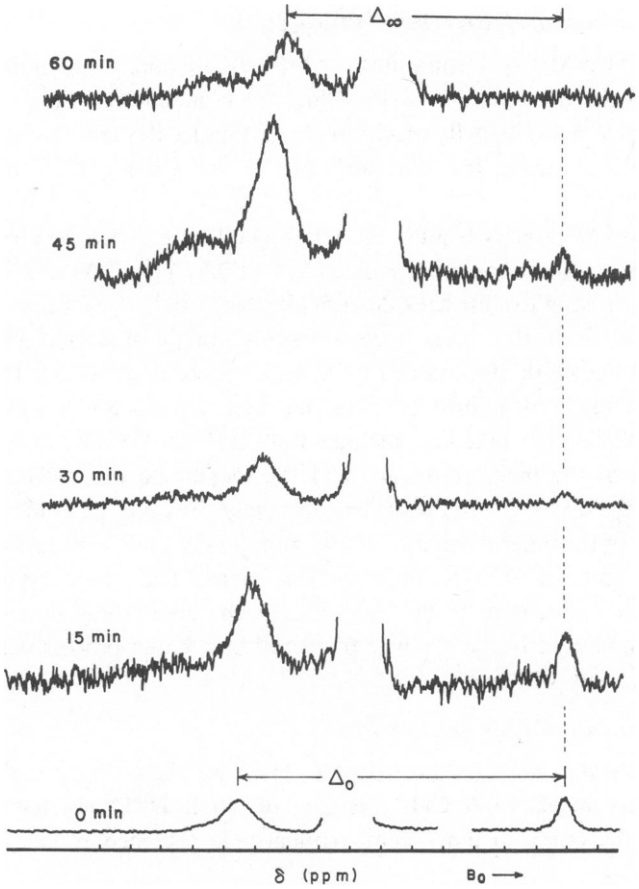

FIGURE 2 ^{31}P-NMR spectra (40.5 MHz) of the resonication of DPL vesicles in D_2O at 50°C. DPL concentration is 70 mM. At t = 0, $Pr(NO_3)_3$ was present only in the intervesicular aqueous space; $[Pr^{+3}]$ = 8 mM. Total elapsed resonication times are given. Salt (140 mM sodium dimethyl phosphate) was also present in all aqueous spaces. The dimethyl phosphate resonance is omitted for clarity. The vertical scales in the different spectra are not the same. The data are taken from the work of Chrzeszczyk (1978).

[Chrzeszczyk et al., 1976; Chrzeszczyk, 1978]. This also indicates that either the binding constant, the limiting stoichiometry, the headgroup conformation, or some combination of these is different for the inner and outer vesicle surfaces. [Chrzeszczyk, 1978].)

Thus, since no intermediate inner DPL resonances are observed, there are significant amounts of only two kinds of vesicles: those which have received all their 56 Pr^{+3} ions, and those which have received no Pr^{+3} ions. Thus, the loading of the vesicles must involve an all or nothing process. The time course of disappearance of the inner DPL resonance obeys the first order rate law with a $t_{1/2}$ of 12 min (Chrzeszczyk, 1978), but we surmise that these kinetics must primarily depend upon the sonicator power setting. Others have also reported an all or nothing process for the ionic equilibration of inner and outer vesicular compartments mediated by ultrasonic irradiation (Lawaczeck et al., 1976).

The "Slow Leakage" Process

Fig. 3 depicts the ^{1}H-NMR spectrum, in the $-N(CH_3)_3$ region, of small dimyristoyl-lecithin (DML) vesicles as the translocation of Eu^{+3} ions from outside to inside is mediated by the presence of 7.4 mol % γ-myristoyllysolecithin (MLL) molecules incorporated into the vesicle bilayers. These data are taken from the work of Lee and Chan (1977) and Lee and Chan, unpublished results.

Before the transport process begins, the outer DML and MLL headgroup resonance is shifted upfield relative to the inner resonance ($\Delta_0 = +0.17$ ppm). As the transport proceeds, the outer resonance is seen to shift back downfield exponentially with time.

The inner resonance, in this case, moves smoothly upfield and itself approaches its final chemical shift and linewidth asymptotically. In its final position, observed at 3,500 min (not shown), it is completely indistinguishable from the outer resonance at +0.15 ppm. At the final equilibrium, each vesicle has taken an average of 49 Eu^{+3} ions inside. The smooth change of the chemical shift of the inner resonance and the monotonic time course of its linewidth change mean that the 49 Eu^{+3} ions are leaking in slowly: only one or, at most, a few at a time. The chemical shift of the inner resonance at 269 min, +0.06 ppm, for example, means that all the vesicles have received ~20 of their 49 Eu^{+3} ions. This same type of behavior for lysolecithin mediated transport of Pr^{+3} has also been reported by others (Bergelson and Bystrov, 1975) and is exactly the opposite of the all or nothing process described above. Its mechanistic implications will be discussed later.

The Intermediate Transport Process

A third type of behavior is exhibited in Fig. 4. Here we show the time dependence of the ^{1}H-NMR spectrum, in the $-N(CH_3)_3$ region, of small DPL vesicles as Pr^{+3} ions are transported from the outer to inner compartments via the mediation of the ionophorous antibiotic A-23187.

Before the transport process begins, the outer DPL headgroup resonance is downfield from the inner resonance ($\Delta_0 = -0.39$ ppm). As the transport proceeds, the outer resonance is seen to shift back upfield exponentially with time (Δ_∞ is $\simeq -0.29$ ppm).

In contrast to the above results, the inner resonance quickly becomes extremely broad and loses some intensity while shifting at the same time. Eventually, when an average of ~120 Pr^{+3} ions have entered each vesicle, it sharpens back up again at its equilibrium position, indistinguishable from the outer resonance. This behavior must mean that during the course of the transport different vesicles are gaining internal Pr^{+3} ions at vastly different rates. The mechanistic implications of this will be discussed later. Hunt has depicted similar behavior for A-23187-mediated transport (Hunt, 1975, Hunt et al., 1978) as has Chen for X-537A-mediated transport (Chen, 1978).

In the next section we will present a kinetic model which encompasses the broad range of transport behavior exhibited above.

THEORY (A KINETIC MODEL)

Continuous Flow Model

Let us first briefly consider the ion transport from the point of view of a continuous flow. We define: $T_{out} \equiv [Ln^*]_{out}$ and $T_{in} \equiv [Ln^*]_{in}$, where the square brackets represent stoichiometric

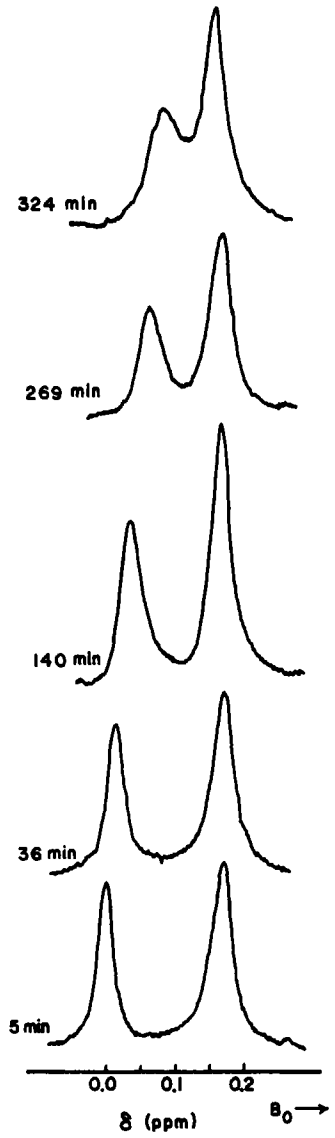

FIGURE 3

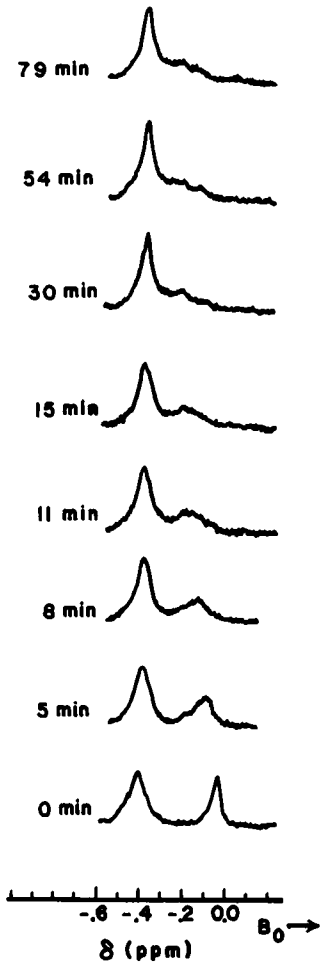

FIGURE 4

FIGURE 3 ^{1}H-NMR spectra (220 MHz) of lysolecithin-mediated Eu^{+3} transport into DML vesicles in D_2O at 50°C. Vesicles contained 7.4 mol % myristoyllysolecithin (MLL). At t = 0, the inner aqueous spaces contained 10 mM La^{+3} while the intervesicular aqueous space contained 5mM La^{+3} and 5 mM Eu^{+3}. The data are taken from the work of Lee and Chan (1977).

FIGURE 4 ^{1}H-NMR spectra (220 MHz) of efrapeptin (A-23187)-mediated Pr^{+3} transport into DPL vesicles in D_2O at 53.5°C. DPL concentration is 33.28 mM and aqueous phase contains 12.88 mM Tris buffer, pD = 8. At t = 0, A-23187 was introduced to intervesicular aqueous space (230 μM) which was 4.0 mM in La^{+3} and 5.3 mM in Pr^{+3}; the inner aqueous spaces contained 10.7 mM La^{+3}.

concentrations. Since we will be developing a vesicular-based model, the units of these concentrations are ions/Å^3. The net flux of Ln* into an average vesicle, J^* [in ions/(Å^2 · s)], is defined by Eq. 1, where V_{in} is the volume of the inner aqueous compartment in Å^3, and A is the area of the membrane center in Å^2 (see Fig. 1):

$$\frac{dT_{in}}{dt} = \left\{\frac{A}{V_{in}}\right\} \cdot J^* \tag{1}$$

(Hunt et al., 1978). But, from Fick's first law of diffusion, we can write Eq. 2, where P^* is the transmembrane tracer permeability coefficient in

$$J^* = P^*_{in}T_{out} - P^*_{out}T_{in} \tag{2}$$

Å/s, and the subscripts in and out are used to indicate the direction of flow into and out of the vesicle, respectively. (The quantities P^*_{in} and P^*_{out} need not be equal; consider the case of active transport. If they are not equal, then at steady state [$J^* = 0$], T^f_{in} will not equal T^f_{out}.) Recalling our use of $\langle Z_{eq}\rangle$ earlier, we now introduce Z as the number of Ln* ions which have entered the average vesicle at any time t. Letting $T_{in} = Z/V_{in}$, Eq. 1 can be written in terms of Z and its steady-state value, Z^f, (Eq. 3) where V_{out} is the intervesicular aqueous

$$\frac{dZ}{dt} = -\left\{\frac{AP^*_{in}}{V_{out}} + \frac{AP^*_{out}}{V_{in}}\right\}(Z - Z^f);\ Z(t = 0) = 0 \tag{3}$$

volume. Upon integration, we obtain the result (see Sjodin, 1971):

$$Z = Z^f\left\{1 - \exp\left[-A\left(\frac{P^*_{in}}{V_{out}} + \frac{P^*_{out}}{V_{in}}\right)t\right]\right\}. \tag{4}$$

The above derivation assumes that the transport process is smooth (continuous) in time. Accordingly, Z is a well-behaved function of time (exponential). This assumption is necessarily an approximation. As we examine the transport process with finer time resolution, we must consider its stochastic nature. We now investigate this aspect.

Stochastic Flow Model

Strickly speaking, we must describe the transport process for an arbitrarily chosen vesicle by a stochastic differential equation, analogous to Eq. 3 where the rate constant in Eq. 3 is replaced by $\beta(t)$, a random function of time:

$$\frac{dZ}{dt} = -\beta(t)(Z - Z^f);\ Z(t = 0) = 0. \tag{5}$$

If necessary, the "systematic" term on the right hand side of Eq. 5 could be augmented by the addition of a "fluctuating" term, thus allowing for a "noisy" approach of Z to its final value. One might also note the similarities to the fluctuational and relaxational analyses of BLM conductance experiments (Neher and Stevens, 1977). The random process, $\beta(t)$, is obviously the quantity of prime interest here. It describes the mediated vectorial transport of ions into the vesicle. An arbitrarily chosen time course might appear as in Fig. 5.

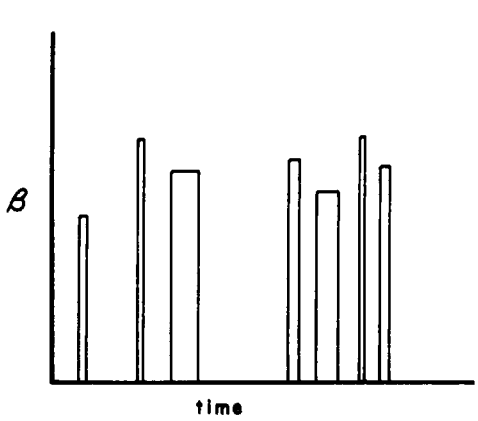

FIGURE 5

Stochastic differential equations of the form of Eq. 5 have been widely studied (Van Kampen, 1976). The formal solution for any given $\beta(t)$ is

$$Z(t) = Z^f\left[1 - \exp\left(-\int_0^t \beta(t')\,dt'\right)\right]. \tag{6}$$

Since $\beta(t)$ is a random function of time, Eq. 6 serves to define the properties of $Z(t)$ in terms of those for $\beta(t)$ and we can calculate $Z(t)$ analytically only if we are given an explicit form for $\beta(t)$. However, if $\beta(t)$ truly represents a random process, each vesicle in an ensemble will have a different and unpredictable form for $\beta(t)$. Thus, we can deal only with the statistics of the ensemble of all vesicles.

The ensemble average of $Z(t)$, $\langle Z(t)\rangle$, is given in Eq. 7.

$$\langle Z(t)\rangle = Z^f\left\{1 - \left\langle \exp\left[-\int_0^t \beta(t')dt'\right]\right\rangle\right\} \tag{7}$$

The averaged exponential term on the right hand side of Eq. 7 is well approximated by Eq. 8 (Van Kampen, 1976). The quantity β_{eff} can be evaluated in terms of the

$$\left\langle \exp\left(-\int_0^t \beta(t')dt'\right)\right\rangle = e^{-\beta_{eff}t} \tag{8}$$

cumulants of $\beta(t)$ and is a time-independent constant, to any order of approximation, as long as $\beta(t)$ is stationary and one observes the ion transport at times t sufficiently greater than the characteristic time of the correlation function of $\beta(t)$. The significance of this result is that the average value of $Z(t)$ exhibits an exponential time dependence, as shown in Eq. 9. This result permits one to relate the stochastic flow treatment for an ensemble of vesicles (Eq. 9) and the continuous flow

$$\langle Z(t)\rangle = Z^f[1 - e^{-\beta_{eff}t}] \tag{9}$$

treatment for a single average vesicle (Eq. 4). We obtain

$$A\left\{\frac{P^*_{in}}{V_{out}} + \frac{P^*_{out}}{V_{in}}\right\} = \beta_{eff}. \tag{10}$$

Idealized Single Vesicle

To a first order of approximation, β_{eff} is equal to the ensemble average of $\beta(t)$, $\langle\beta(t)\rangle$, even for infinitely short times. We imagine a hypothetical "idealized" vesicle with average properties, i.e., one which exhibits a regular pulsatile time course for $\beta(t)$ and a time averaged value of $\beta(t)$ equal to $\langle\beta(t)\rangle$. Then, if β_0 is the height of the regular pulses, t_p the duration, and γ the number of pulses per unit time; $\langle\beta(t)\rangle = \beta_0 t_p \gamma = \beta_{eff}$. Now, if we let each pulse define a "mediating event," then for an idealized vesicle with such a time course, the number of mediating events having occurred after time t, N, is given by γt. The product $\beta_0 t_p$ is simply the area under a pulse, ρ, and since we will not generally be able to separate the factors in this product, we shall henceforth consider this quantity only. It is dimensionless since β has dimensions of t^{-1} (Eq. 5). Thus, for our idealized vesicle, we have

$$Z(t) = Z^f(1 - e^{-\rho N}). \tag{11}$$

One interesting way of ascertaining the effect of ρ can be seen by extrapolating Eq. 11 back to the situation after one event (i.e., $N = 1$). (One might worry about the validity of Eq. 11 at a time short enough for only one event to have occurred. However Eq. 11 is only a first order approximation to Eq. 9. The stipulation of long times being required for Eq. 9 is only necessary for higher order approximations. See the discussion of Eq. 8 above.) We obtain Eq. 12,

$$z/Z^f = 1 - e^{-\rho}, \tag{12}$$

where z is the number of Ln* ions which enter during the first event. It is clear that ρ is an exponential measure of z/Z^f, the relative "efficiency" of the first event. If $\rho = 5$, $z/Z^f = 0.99$ and the transport is essentially complete after the first event. If $\rho = 0.01$, $z/Z^f = 0.01$ and it will take many events for the transport to be completed. The overriding significance of this will become evident later. We will show in the Discussion that a calculation of ρ using kinetic parameters experimentally determined for a process thought to proceed via mobile carrier mediation leads to a small ("inefficient") value of ρ, while a similar calculation for a process thought to occur via pore mediation leads to a large value of ρ.

NMR Spectrum of the Inner Headgroup Resonance of a Single Vesicle

Since the lanthanide ion/membrane binding kinetics inside a vesicle are certainly also fast on the NMR time scale, the chemical shift, ν_0, as well as the full linewidth, at half height, Γ, of the inner headgroup resonance of the vesicle is proportional to the number of Ln* ions which have become transported to the inside, Z. This proportionality is linear if we retain our assumption that the linear region of the NMR binding isotherm obtains. The quantity Z depends, in turn, on N. Thus, we can write Eq. 13 where C and C' are proportionality constants which depend on

$$\nu_0(N) = CZ + \nu_0^s, \Gamma(N) = C'Z + \Gamma^s, \tag{13}$$

the nature of the lipid and Ln* and which vary inversely as the size of the vesicle. When $N = 0$, $Z = 0$, and thus $\nu_0(0) = \nu_0^s$ and $\Gamma(0) = \Gamma^s$. When $Z = Z^f$, $\nu_0^f = CZ^f + \nu_0^s$ and $\Gamma^f = C'Z^f + \Gamma^s$.

For passive transport down the isomorph gradient, $Z^f = Z_{eq}$. Combining Eqs. 11 and 13 and using the above notation, we obtain Eq. 14:

$$\frac{\nu_0(N) - \nu_0^f}{\nu_0^s - \nu_0^f} = e^{-\rho N}, \frac{\Gamma(N) - \Gamma^f}{\Gamma^s - \Gamma^f} = e^{-\rho N}. \tag{14}$$

To a first order of approximation, and for an idealized vesicle, the inner headgroup NMR line position and width are exponentially determined by the product of the average area under a transport pulse and the number of pulses which have occurred. (The chemical shift and linewidth of the outer headgroup resonance should follow an analogous time course. Thus, for example, $\Delta_t = [e^{-\rho N}(\Delta_0 - \Delta_\infty)] + \Delta_\infty$.) The homogeneous resonance of a single vesicle will have a Lorentizian line shape given by Eq. 15. The quantities $\Gamma(N)$ and $\nu_0(N)$ require us to know a value for N

$$L_N(\nu) = \frac{2\Gamma(N)/\pi}{[\Gamma(N)]^2 + 4[\nu - \nu_0(N)]^2}, \tag{15}$$

but, as we have seen, the occurrence of events is a random process continuous in time. Thus, all we can state is the probability of N events having occurred after time t, $p(N)$, and this only if we know the probability distribution of N. It is known, however, that for random pulses the probability is given by the Poisson distribution function where $\overline{N}$ is the expected number of events after time t (Heer, 1972).

$$p(N) = \frac{\overline{N}^N \cdot e^{-\overline{N}}}{N!}. \tag{16}$$

We postulate that the expected number of events in an idealized vesicle is related to the elapsed time via the previously introduced proportionality constant, γ, and also some function of M, the number of mediators (or mediating species) present in the vesicle membrane and m, the "molecularity" of the mediating event.

$$\overline{N} = \gamma \cdot f(M, m) \cdot t. \tag{17}$$

If we assume no specific interactions between mediating species, $f(M, m) = \left|\begin{matrix} M \\ m \end{matrix}\right|$, the number of combinations of M mediators, taken m at a time. The quantities γ, ρ, and m represent the

$$\overline{N} = \gamma \left|\begin{matrix} M \\ m \end{matrix}\right| t. \tag{18}$$

three adjustable parameters introduced into our kinetic model. The first order rate constant, γ, embodies the temperature and pressure dependence of the transport process. The average pulse area, ρ, has already been discussed. The third parameter, m, represents the number of mediators in a functioning complex if there is only one kind of functioning complex; otherwise m represents some weighted average of the molecularities of the various complexes. Employing the standard expression for $\left|\begin{matrix} M \\ m \end{matrix}\right|$, we obtain Eq. 19.

$$\overline{N} = \frac{\gamma M! t}{m!(M - m)!}. \tag{19}$$

In the limit that $M \gg m$, $\left|\begin{matrix} M \\ m \end{matrix}\right|$ approaches the familiar concentration dependence of a kinetic

rate law, M^m. Large values of m would imply specific interactions between mediating species and thus the $\binom{M}{m}$ approximation may break down in such a case. Combining Eqs. 16 and 19, we obtain Eq. 20:

$$p(N) = \frac{\left[\frac{\gamma M! t}{m!(M-m)!}\right]^N \exp - \left[\frac{\gamma M! t}{m!(M-m)!}\right]}{N!}. \tag{20}$$

This equation expresses the fact that the spread of probabilities is significant at times short compared to the magnitude of γ^{-1}. Only at longer times does the probability begin to center sharply on $\overline{N}$ (in terms of relative width).

NMR Spectrum of the Inner Headgroup Resonances of the Ensemble of Vesicles

We now wish to simulate the spectrum of the observed inner headgroup resonance. Since it reflects contributions from all the vesicles present in the sample we must consider the ensemble of vesicles. We can do this by constructing a model ensemble of idealized vesicles. The more monodisperse the experimental vesicle size distribution, the better the interpretative quality of our model. However, since we only deal with the average values of distributed quantities (γ, ρ, m, $\overline{N}$, and $\overline{M}$; see below) and assume statistical distribution widths, polydispersity does not have to enter explicitly. Application to real data (see below) indicates that, even with uncritical sample preparation, this is not an overwhelming problem.

During the course of a transport study the lipid concentration, and thus (assuming no fusion) the vesicle concentration, remains constant. In this case, the observed spectrum $I(\nu)$ for the inner headgroup resonance at any given time t is a superposition of Lorentzians of all of the vesicles with different values of Z, weighted according to the normalized probability of a vesicle having that value of Z, $p(Z)$, where $p(Z)$ is time-dependent. Depending upon the value of N for a specific vesicle at time t, the value of Z will vary and the contribution of this vesicle to $p(Z)$ will be different. If all vesicles had the same number of mediators, M, the spectrum would be simply given by

$$I(\nu) = \sum_N L_N(\nu) \cdot p(N). \tag{21}$$

The time-dependent distribution $p(N)$ thus serves to give us our model ensemble of vesicles.

However, we recognize that M itself will also be a distributed quantity and that vesicles with different numbers of mediators will undergo N mediating events at different times after the onset of the ion transport experiment. Thus, the width of the distribution function $p(Z)$ is determined by both $p(N)$ and $p(M)$, where $p(M)$ is the probability of a vesicle having M mediators. The quantity M is itself an integral-valued random variable and since its value is usually quite small compared to the average number of lipids per vesicle (~3,000 for most preparations [Chrzeszczyk et al., 1977]), $p(M)$ for an equilibrated system is also correctly given by the Poisson distribution:

$$p(M) = \frac{e^{-\overline{M}} \cdot \overline{M}^M}{M!}. \tag{22}$$

The quantity $\overline{M}$, the average value of M, can be calculated as the product of the

stoichiometric molar ratio of mediator to phospholipid and the average vesicle aggregation number if the mediator partitions completely into the vesicle membranes.

The nature of the combination $\left|\begin{matrix} M \\ m \end{matrix}\right|$, which is needed for Eq. 18, depends upon the dynamics of intervesicular mediator exchange. We recognize three distinct cases.

A. MEDIATOR EXCHANGE NONEXISTENT DURING ENTIRE COURSE OF ION TRANSPORT In this case, we can consider $M \neq M(t)$. This is likely to be the situation for protein mediators. The spectrum will be given by Eq. 23,

$$I(\nu) = \sum_{M} \sum_{N} L_{N_M}(\nu) \cdot p(N_M) \cdot p(M), \tag{23}$$

where we have rewritten the Lorentzian function of Eq. 15 as $L_{N_M}(\nu)$, the Lorentzian for an idealized vesicle with M mediators which has undergone N events, and $p(N)$ of Eq. 20 as $p(N_M)$. The relative width of $p(N_M)$ decreases with increasing time elapsed, and hence $p(M)$ should dominate the spread in Z at sufficiently long times if $\overline{M}$ is reasonably small (see Results). In practice this leads to broadening of the composite spectrum at intermediate times as a result of the distribution in the rates in which the ions are transported into the vesicles. It corresponds to a temporary "kinetic" broadening (see Figs. 4 and 9). Combining Eqs. 14, 15, 20, and 22, we write the complete form of Eq. 23 as

$$I(\nu) = \sum_{M} \sum_{N} \frac{\{2[e^{-\rho N}(\Gamma^s - \Gamma^f) + \Gamma^f]/\pi\} \cdot \left\{\frac{\left[\frac{\gamma M! t}{m!(M-m)!}\right]^N \cdot \exp - \left[\frac{\gamma M! t}{m!(M-m)!}\right]}{N}\right\} \cdot \left\{\frac{\overline{M}^M \cdot e^{-\overline{M}}}{M!}\right\}}{[e^{-\rho N}(\Gamma^s - \Gamma^f) + \Gamma^f]^2 + 4\{\nu - [e^{-\rho N}(\nu_0^s - \nu_0^f) + \nu_0^f]\}^2}. \tag{24}$$

In this equation, which describes the time evolution of the line shape for the inner headgroup resonance, ν_0^s, ν_0^f, Γ^s, Γ^f, and the upper limit of $\overline{M}$ are measurable constants in any given experiment. The quantities ν and t are independent variables: γ, m, and ρ are the parameters to be determined experimentally.

B. MEDIATOR EXCHANGE VERY FAST COMPARED TO ION TRANSPORT For any case other than A we must replace the M in Eq. 18 by $M(t)$. For the limiting case where mediator exchange is very fast, compared to ion transport, the value of M is effectively the same for all vesicles. It is given by the time average of $M(t)$ which, in this case, is the same as the ensemble average. Assuming that the only time vesicles transport ions is when the value of M is greater than m, we write

$$\left\langle \left| \begin{matrix} M(t) \\ m \end{matrix} \right| \right\rangle_t = \sum_{M=m}^{\infty} \left| \begin{matrix} M \\ m \end{matrix} \right| \cdot p(M). \tag{25}$$

Substituting the standard expression for $\left|\begin{matrix} M \\ m \end{matrix}\right|$, the distribution function for $p(M)$, Eq. 22, and simplifying, we obtain

$$\left\langle \left| \begin{matrix} M(t) \\ m \end{matrix} \right| \right\rangle_t = \frac{\overline{M}^m}{m!}. \tag{26}$$

This changes the form of Eqs. 19 and 20, and, since all idealized vesicles have effectively the same value of M, we can use Eq. 21 as our line shape equation. It is reexpressed as

$$I(\nu) = \sum_N \frac{\{2[e^{-\rho N}(\Gamma^s - \Gamma^f) + \Gamma^f]/\pi\} \cdot \left\{\frac{\left[\frac{\gamma \overline{M}^m t}{m!}\right]^N \cdot \exp - \left[\frac{\gamma \overline{M}^m t}{m!}\right]}{N!}\right\}}{[e^{-\rho N}(\Gamma^s - \Gamma^f) + \Gamma^f]^2 + 4\{\nu - [e^{-\rho N}(\nu_0^s - \nu_0^f) + \nu_0^f]\}^2}. \quad (27)$$

C. MEDIATOR EXCHANGE OCCURS AT ABOUT THE SAME RATE AS ION TRANSPORT This is the most complicated situation and we have not derived an analytical line shape equation analogous to Eq. 24 or Eq. 27 in this work. We have simulated this case with a Monte Carlo calculation which we will describe in a separate publication.

RESULTS

Slow Mediator Exchange

We have written a computer program called VESICL based on Eq. 24 which calculates and plots the NMR spectrum of the inner headgroup resonance under the condition of no mediator exchange (Appendix A). We have investigated the effects of the magnitudes of the parameters ρ, $\overline{M}$, and m on the observed spectrum.

THE EFFECTS OF ρ As pointed out above, ρ can be thought of as the average area per mediating pulse. It is dimensionless and is a nonintegral-valued variable which itself has a time-dependent distribution $p(\rho)$. It could quite possibly also be a function of m but, for the purpose of this discussion, we will use only the average value of this distribution. Its role as a measure of relative efficiency can perhaps be more easily appreciated from the following.

We have already indicated that when $\rho > 5$, $z \simeq Z^f$. Putting such a value of ρ into the chemical shift Eq. 14, for $N = 1$, gives us $\nu_0(1) \simeq \nu_0^f$. This is exactly the condition for the observation of an all or nothing process. The inner headgroup resonance jumps from ν_0^s to ν_0^f without ever going through any intermediate frequencies. An example is shown in Fig. 6 *a* where the time course of an inner resonance is shown when $\rho = 5.00$. The presence of an all or nothing process can be operationally defined by the observation of a single isosbestic point when the spectra are overlaid. The values of the other parameters are given in the figure caption. The values of Γ^s (10 Hz), Γ^f (20 Hz), ν_0^s (+30 Hz), and ν_0^f (+140 Hz) are the same for Fig. 6–8. The value of ν_0^f is appropriate for an upfield shift reagent, for example, Eu^{+3}.

Consider now a smaller value of ρ, for example 0.63. The quantity z/Z_{eq} will be equal to 0.47. This gives rise to a different kind of time course for the inner headgroup resonance (Fig. 6 *b*). As time progresses, one sees new peaks growing in at frequencies which are given by the exponential series $e^{-\rho N}(\nu_0^s - \nu_0^f) + \nu_0^f$. For the values of ν_0^s and ν_0^f used in Fig. 6 *b*, these frequencies are +81, +109, +123, etc. (N = 1, 2, 3, etc.). The various spectral lines do not shift with time but only change intensities ("standing waves"). Thus, one can "see" simultaneously vesicles which have suffered none, one, two, etc. events. This might be called a "something or nothing" process.

Fig. 6 *c* depicts the situation when $\rho = 0.2$. In this case, one can barely distinguish the resonances of the vesicles which have experienced one, two, and three events at +50 Hz, +66 Hz, and +80 Hz, respectively. Also, the exponential series converges at much smaller

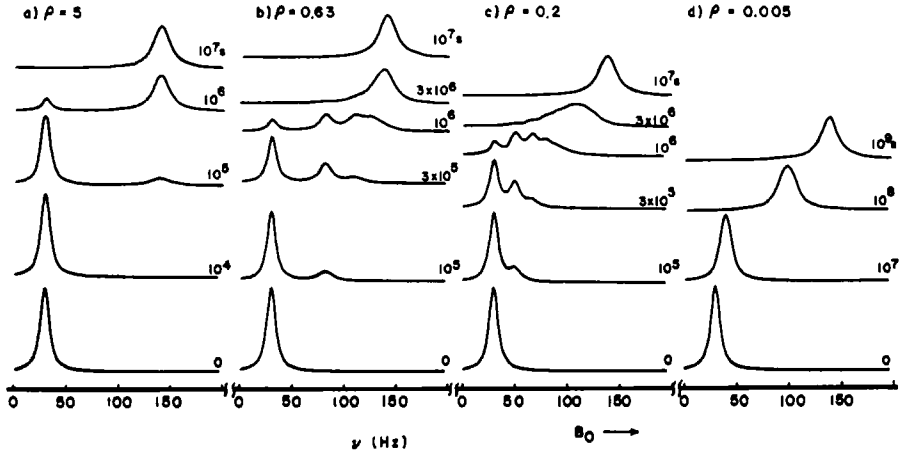

FIGURE 6 Simulated time evolutions of inner headgroup NMR spectra (Eq. 24). The effect of the magnitude of ρ. In all spectra, $\overline{M} = 200$, $m = 2$, and $\gamma = 10^{-8}$.

hyperfine shifts. Lines this close together would probably prove hard to resolve experimentally and could give rise to an apparent intermediate broadening. (However, see the simulations of literature spectra below.)

Now, let us consider very small values of the parameter ρ; i.e., as it approaches zero. Since the efficiency of each event is so small, the inner headgroup resonance will move along the chemical shift scale in such small jumps that its motion will appear continuous. This is shown in Fig. 6 *d* where $\rho = 0.005$. This is one, but not the only (see below), condition for the observation of a "slow leakage" process.

THE EFFECTS OF $\overline{M}$ The quantity $\overline{M}$ is the average number of mediating species per vesicle. For the variation of ρ in Fig. 6, the magnitude of $\overline{M}$ was held constant at 200. When $\overline{M}$ is this large, the contribution of the breadth of p(M) to the breadth of the spectrum (Eq. 23) is small. The large value of $\overline{M}$ dominates and makes all values of $\overline{N}$ large (Eq. 19) irrespective of the values of γ and t. This is illustrated in Fig. 7 *a*, where $\overline{M}$ is again 200. Since ρ is also small, 0.01, slow leakage behavior is apparent. However, for smaller values of $\overline{M}$, intermediate broadening caused by the breadth of $p(M)$ can be rather dramatic. This condition will be most evident when $\overline{M}$ is small and will be exaggerated by large values of m. We have demonstrated the former in the rest of Fig. 7, where $\overline{M}$ becomes progressively smaller (from 200 to 2). As $\overline{M}$ becomes smaller, intermediate broadening is observed (Fig. 7 *b*). This can obviously be carried to such an extreme when $\overline{M}$ is very small, a common situation with protein mediators, that resolvable "travelling waves" from different vesicles are observed. This is demonstrated in Fig. 7 *c*, where $\overline{M}$ is 2. The spectrum at 3,000 s exhibits four resolvable peaks. These can probably be assigned, from right to left, to vesicles with 4 and 3, 2, 1, and 0 mediators, respectively. When the reaction is essentially complete, at 30,000 s, there is still a peak remaining in the unshifted position. This corresponds to the vesicles with zero mediators. Recall that the model we are using here assumes that no mediator exchange occurs. Thus those vesicles which have no mediators can never take up any Ln* ions. (If similar simulations, i.e., with small $\overline{M}$, are run, but with larger values of ρ, spectra similar to

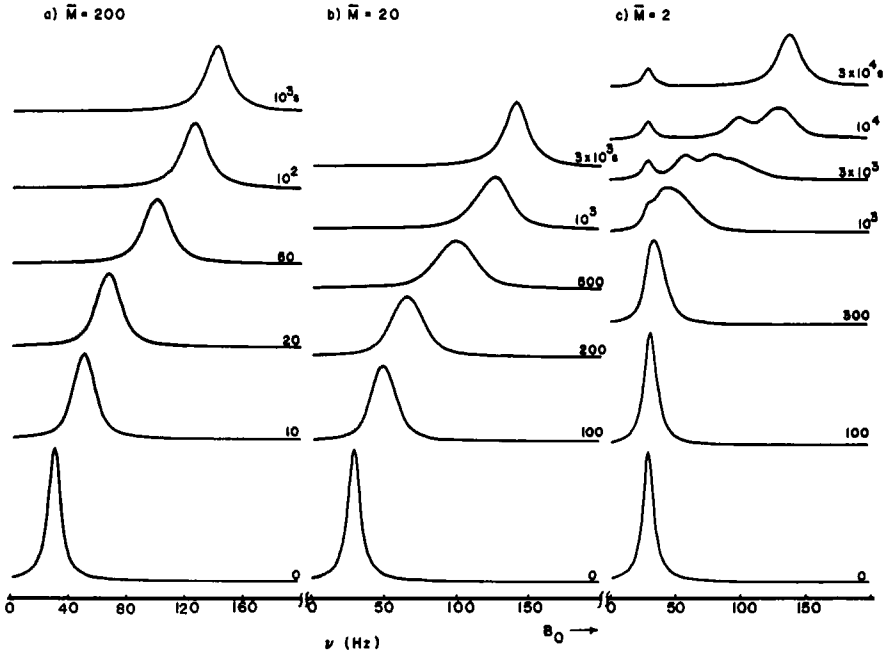

FIGURE 7 Simulated time evolutions of inner headgroup NMR spectra (Eq. 24). The effect of the magnitude of $\bar{M}$. In all spectra, $\rho = 0.01$, $m = 1$, and $\gamma = 0.01$.

those Fig. 6 *a* or *b* are observed except that a small peak always remains at the unshifted position.) We will demonstrate the effects of mediator exchange in a separate paper. In any case, it is now clear that the elaboration of slow leakage behavior requires both small ρ and moderately large $\bar{M}$ to obtain in cases where mediator exchange is slow or nonexistent.

THE EFFECTS OF m Larger values of the parameter m, the molecularity of the mediating complex, can exaggerate both the intermediate broadening caused by small values of $\bar{M}$ and the travelling waves caused by very small values of $\bar{M}$. The former point is illustrated in Fig. 8, where a systematic variation of m is made. The values of $\bar{M}$ and ρ are held constant at 10 and 0.005, respectively, so that the situation of a small number of inefficient mediators is simulated. When $m = 1$ (Fig. 8 *a*), the spectra are very similar to those in Fig. 7 *b*, that is, moderate intermediate broadening is observed. However, as m is increased (two in Fig. 8 *b* and four in Fig. 8 *c*), the intermediate broadening becomes extremely exaggerated. Note, for example, the spectrum at 300 s in Fig. 8 *c*: the inner headgroup resonance seems to have almost disappeared. It is also interesting to note that, in simulations with very small values of $\bar{M}$, not only does the variation of m greatly exaggerate the travelling waves (when ρ is small) but it also changes the fractional area of the inner resonance which remains unshifted (Fig. 7 *c*). This is because all vesicles with values of $M < m$ cannot translocate ions in our model. For example, with $\bar{M} = 2$, when $m = 1$, (Fig. 7 *c*) only 14% of the vesicles cannot translocate ions, while when $m = 2$, 41% cannot. This probably is an important diagnostic property for actual cases of nonexchanging mediators (see Discussion).

THE EFFECTS OF γ We have not performed any computations for the variation of the rate constant parameter γ, the mean time between mediating pulses. For our isothermal,

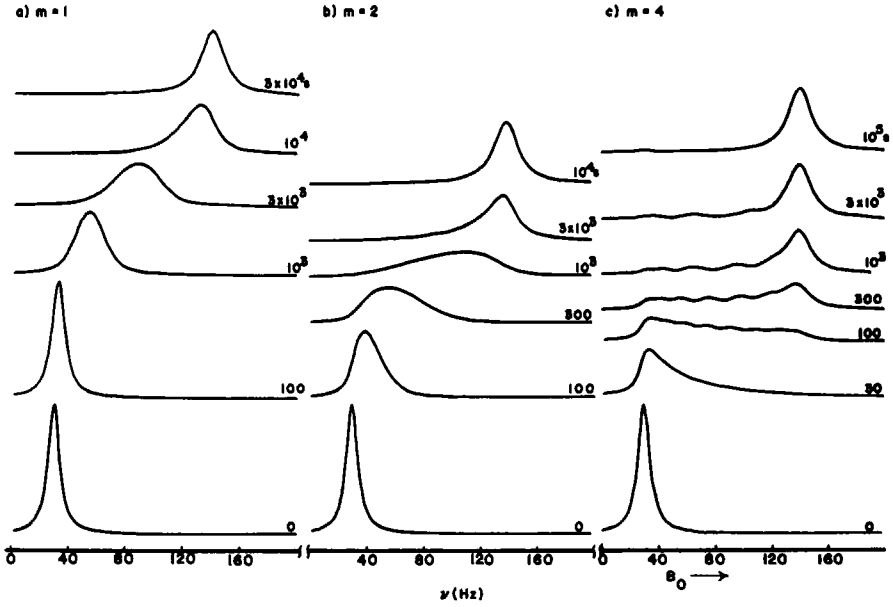

FIGURE 8 Simulated time evolutions of inner headgroup NMR spectra (Eq. 24). The effect of the magnitude of m. In all spectra, $\overline{M} = 10$, $\rho = 0.005$, and $\gamma = 0.005$.

isobaric theoretical calculations, it is simply a scaling factor for t. It cannot change the shape of the simulated spectra. However, as mentioned before, γ, would contain the temperature and pressure dependence of the ion transport reaction.

Intermediate and Fast Mediator Exchange

It is intuitively clear and we have found in unpublished computer simulations that mediator exchange can broaden out the fine structure observed in Figs. 6–8, giving rise to intermediate broadening, and, in the fast exchange limit (where Eq. 27 would become the proper analytical expression), a slow leakage appearance.

DISCUSSION

We have shown that our kinetic model can account for the range of spectral behavior already observed in NMR cation transport studies and that it predicts some new spectral responses not yet observed. These are most evident in the limiting case of no mediator exchange, which should be appropriate for protein mediated transport.

Most dramatic is the all or nothing process. As we have seen, this is characterized by a high efficiency per event (ρ). This was exemplified by ion transport mediated by ultrasonic irradiation, which is assumed to cause vesicles to disintegrate into many lipid aggregate components. When these reform to create a new vesicle the inner aqueous compartment would obviously be completely equilibrated. More interesting is the idea that this should be the manifestation of the operation of an efficient "pore" mechanism for a mediated transport process. A calculation in Appendix B gives an "experimental" value of ρ to be 3,500 for a

transport process thought to occur via a pore mechanism. Obviously, this is more than enough to exhibit all or nothing behavior in an NMR experiment.

All or nothing behavior has been reported for the annealing of structural defects artifically created by sonication below the lipid T_c (Lawaczeck et al., 1976), and for thermally induced transport at T_c in pure lipid bilayers (Lawaczeck et al., 1977; Hunt, 1980), in bilayers containing cholesterol or hexadecane (Hunt and Tipping, 1978), and in bilayers containing Triton X-100 (Hunt, 1980). Such behavior is implied also by Cushley and Forrest in their description of the transport of Pr^{+3} into vesicles mediated by large amounts of phytanic acid, vitamin E, or phytol (Cushley and Forrest, 1977).

A slightly less efficient pore mechanism would give rise to the something or nothing behavior of Fig. 6 *b*. This spectral behavior has been clearly observed only very recently (after completion of this work): for the chenodeoxycholate-mediated transport of Pr^{+3} into cholesterol-containing DPL vesicles (Hunt and Jawaharlal, 1980). The lack of its common occurrence is likely due to the fact that, for small vesicles, Z^f is small. Thus, the value of z does not have to be very large before the relative efficiency ρ is great enough to make the event appear as an all or nothing process. Small vesicles (generally formed by sonication), therefore, are very useful in demonstrating the discrete nature of rather inefficient mediating events. On the other hand, larger vesicles (generally formed by carrier dilution) might in some cases have values of Z^f large enough such that something or nothing processes may be more commonly observed. (However, larger vesicles will have smaller values of C and C' and larger values of Γ^s [Eq. 13].) Thus vesicles quantize the solution volume and, to a degree, the size of the quanta can be controlled (Szoka and Papahadjopoulos, 1980). In this sense, the small inner aqueous cavity of the sonicated vesicle, previously thought to be a serious disadvantage, can be considered as an amplifying factor for the (normally insensitive) NMR response to the transport of a small number (often, considerably less than 100) of cations across a bilayer membrane. The something or nothing behavior can be considered as the NMR analog of the "current jumps" observed in BLM studies of pore mediated transport (Hladky et al., 1974).

O'Brien and co-workers (1977) recently used this NMR method to study the light-induced rhodopsin-mediated transport of Eu^{+3} ions into reconstituted vesicles. Unfortunately, the qualitative nature of the experiment precludes even a distinction between all or nothing or slow leakage behavior, but the success of this preliminary experiment is encouraging. It indicates the feasibility of this approach and lends credence to the idea that many biological systems which can transport Ca^{+2} can also transport trivalent lanthanide ions.

The slow leakage behavior is a manifestation of a mechanism which has a low efficiency per event. Thus, this might be expected for a protein flip-flop or diffusive carrier mechanism. If less than one, one, or, at most, a few ions are transported per event, and roughly 100 ions are needed for equilibration, then $\rho \lesssim 10^{-2}$ and no discreteness will be observed. This is true no matter how often the inefficient event occurs. For example, large values of γ can be observed for small-molecule mediated transport; see Appendix C, where "experimental" values of ρ and γ are given for a process thought to occur via a "mobile carrier" mechanism.

Slow leakage results reported for cholate, glycocholate, deoxycholate, chenodeoxycholate (Hunt and Jawaharlal, 1980), taurocholate, and Triton X-100 (Hunt, 1980) mediated transport of Pr^{+3} into DPL vesicles have been attributed to an inverted micelle (aggregation number, ~4) carrier mechanism. However, a small value of ρ does not necessarily reflect a

carrier or flip-flop mechanism. Lee and Chan (1977) have interpreted slow leakage data, exemplified by Fig. 3, in terms of a very inefficient (and also infrequent) pore formation by four aggregated lysolecithin molecules (Lee and Chan, 1977; Lee and Chan, unpublished data). "Travelling waves" were not observed presumably because of the large values of $\overline{M}$ (generally >200) required. The same is true of the similar observations of Bergelson and Bystrov (1975).

Our model has predicted situations where "waves" of vesicles obtaining Ln* ions at different rates may be observed (Fig. 7*c*). This requires reasonably slow mediator exchange, very low mediator levels ($\overline{M} = 2$, in Fig. 7*c*), very small efficiency per event and is exaggerated by reasonably large values of m. The former two should be easily obtainable for protein-mediation.

Diffusive carrier mechanisms have often been postulated for ionophore-mediated ion transport. The A-23187 data presented in this paper (Fig. 4) and by Hunt and co-workers (1978), indeed, shows little clear evidence for discreteness during the transport experiment. However, this is not sufficient to rule out completely a pore mechanism which is reasonably inefficient. The intermediate broadening observed in Fig. 4, also depicted by Hunt, is interesting. We have seen that such broadening can arise from any or all of three sources: the breadth in $p(N)$, when ρ is of an intermediate value (0.2 in Fig. 6*c*); the breadth in $p(M)$, when $\overline{M}$ is small (20 in Fig. 7*b*, 10 in Fig 8; $\overline{M}$ was ~21 for the experiment of Fig. 4); and from an intermediate rate of mediator exchange. Experiments by R. Debus in our laboratory have shown unequivocally that A-23187 exchanges among vesicles rather rapidly. It seems quite likely that Fig. 4 is an example of fine structure being broadened out by an intermediate rate of mediator exchange.

Perhaps most interesting is the recent low field ^{31}P-NMR data (15 HMz) for nystatin mediated Pr^{+3} translocation into EL:dihydroergosterol:dicetylphosphate (DCP) vesicles presented by Pierce and co-workers (1978) and photographically reproduced in Figure 9. In addition to obvious intermediate broadening, clear evidence of a residual unshifted inner resonance is seen. Although Pierce et al. (1978) attribute this to contaminating multilamellar vesicles, it is much more likely due to a fraction of small single wall vesicles which cannot translocate Pr^{+3} ions. Large multilamellar vesicles would not be expected to give rise to the sharp inner ^{31}P resonance observed. This offers strong evidence that nystatin exchange among vesicles is slow relative to ion transport, which is on the order of hours (Fig. 9). (Contrary evidence for exchange of amphotericin B, a related antibiotic, among cholesterol-containing EL vesicles has recently been reported; Van Hoogevest and DeKruijff, 1978.) From the stoichiometry of the solution, $\overline{M}$ could be as great as 30 (based on monomolecular nystatin and assuming 3,000 lipids/vesicle), which would seem large enough for all vesicles to take up ions. However, there is good evidence elsewhere that the mediating species is one of high molecularity. A structure consisting of one or two octameric half-pores has been suggested (DeKruijff and Demel, 1974; Van Hoogevest and DeKruijff, 1978).

We have made cursory simulations of the experimental spectra in Fig. 9 using VESICL in a noniterative manner (i.e., the variables were arbitrarily incremented, one at a time). We find that, holding m fixed at 2, we can achieve reasonable simulations (shown in Fig. 9) only if $\overline{M}$ is quite close to 2.8 (within ±10%). This is consistent with the expected strong specific intermolecular interactions within the half-pores (considered the "mediating species" here)

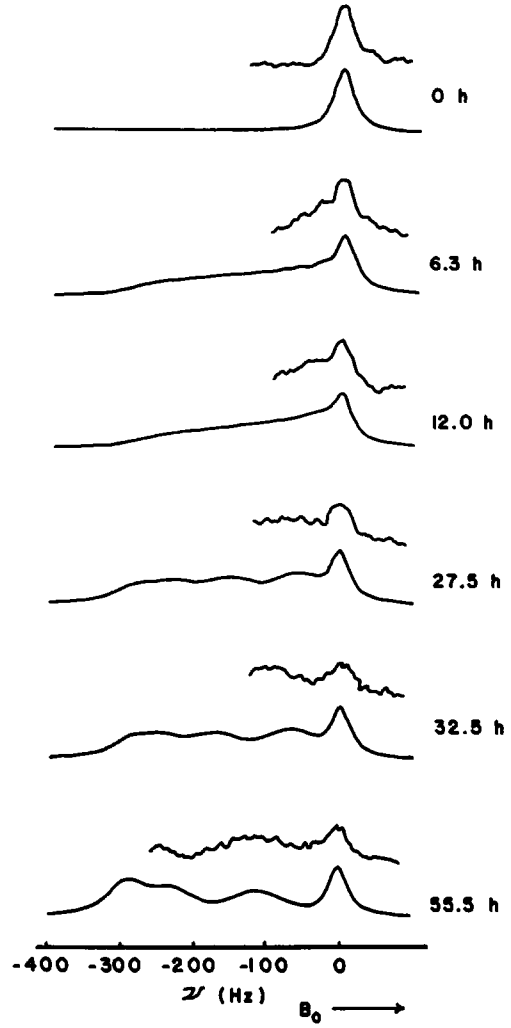

FIGURE 9 Experimental and simulated ^{31}P-NMR spectra (15.1 MHz) of nystatin-mediated Pr^{+3} transport into EL vesicles in H_2O at 37°C. The experimental spectra are the upper members of each pair and represent only the part of the inner surface resonance not distorted by the outer surface resonance. The data are from Pierce et al. (1978), Fig. 4. The EL (0.1 M) vesicles contained 7 mol % DCP and 10 mol % dihydroergosterol and were suspended in 0.05 M Tris buffer, 0.012 M in $Pr(NO_3)_3$ 0. 5 H_2O, and 10^{-3} M in nystatin (added in 100 μL DMF). The simulated spectra are the lower members of each pair. They were simulated with Eq. 24 using $\nu_0^s = 0$, $\nu_0^f = -300$ Hz, $\Gamma^s = 33$ Hz, $\Gamma^f = 57$ Hz, $\overline{M} = 2.8$, $m = 2$, and $\gamma = 0.22$ h^{-1}. The following values for ρ were used: 6.3 h, 0.114; 12 h, 0.05; 27.5, 32.5, and 55.5 h, all 0.04.

and with no particularly specific interactions between half-pores. The half-pores apparently also require one sterol molecule for each nystatin molecule (DeKruijff and Demel, 1974, Van Hoogevest and DeKruijff, 1978). In adddition, our result implies significant partitioning of nystatin into the vesicle membranes (30/8 = 3.7). In terms of the double half-pore model described above, γ would be interpreted as the frequency of encounters involving one half-pore in each monolayer, effective in translocating Pr^{+3} ions. In the simulations shown in Fig. 9, γ

was held constant at 0.22 h^{-1}. Other work also indicates that such pores are infrequently formed in vesicles (Gent and Prestegard, 1976). As expected, the quality of the simulation was found to be quite sensitive to the value of ρ (outside the range 0.15–0.02, the simulations were very poor). The apparent shoulders on the experimental peak at 6.3 h might very well be evidence for discrete transporting events. Ermishkin et al. (1976) have reported current jumps for nystatin in BLM experiments. (The best simulations were found when ρ underwent an initial decrease with time, as shown in Fig. 9). This could be attributable to the build-up of a diffusion potential since the experiments had no transportable cation initially present inside the vesicles. This would increasingly diminish the relative efficiency of the mediating events. Nystatin/sterol pores are anion selective at normal ionic strengths but become nonselective (between K^+ and Cl^-) at low ionic strengths (Finkelstein and Holz, 1973) and could very well become cation selective for trivalent cations at the low ionic strength and with the significantly negatively charged membranes (DCP) of the experiment depicted in Fig. 9. The initial ρ value of 0.114 in the simulations corresponds to a z/Z^f value of 0.11. In the experiment the stoichiometric ratio of Pr^{+3} ions to vesicles was ~360. Assuming that one-fourth of these enter the average vesicle at equilibrium, Z^f is ~90 and z is ~10 ions. That is, the initial mediating events translocate ~10 Pr^{+3} ions each. It seems clear that repetition of this experiment with high-field ^{31}P-NMR spectroscopy (wherein $\nu_0^s - \nu_0^f$ [Eq. 14] could be made considerably larger) and an iterative fitting of Eq. 24 to the resultant data could improve the precision of our understanding of nystatin mediated ion transport considerably. Possibly, a clear distinction between the single half-pore ($m = 1$) and double half-pore ($m = 2$) mechanisms (Van Hoogevest and DeKruijff, 1978) could be made.

The theory presented in this paper, with suitable modification, should be applicable to similar studies where the NMR spectrum of the transported ion itself is monitored. For example, see the recent report by Degani of $^{23}Na^+$-NMR studies of Na^+ transport (Degani and Elgavish, 1978).

APPENDIX A

The program that calculates $I(\nu)$ is straightforward, but it does involve some necessary approximations without which the program would be extremely time-consuming. One approximation was made to improve the efficiency of the calculations of values of the Poisson distribution: (*a*) When $n > 10$, Stirling's formula was used to approximate log $n!$. (The error is 0.04% for $n = 11$, and decreases as n increases.) (*b*) When the mean, $\bar{N}$, of the Poisson distribution is > 5,000, it is approximated by a Gaussian distribution with mean $\bar{N}$ and variance $(N^2 - \bar{N}^2)^{1/2}$ since it involves 3–4 times fewer calculations. (The relative error is 0.005% at the mean and increases to 4% at 3 SD from the mean. This increase in error is inconsequential since the values of the distribution decrease rapidly as we go away from the mean.)

Another approximation was made in the calculation of $\Sigma_N L_N(\nu)p(N)$ (Eq. 21) for a particular ν. Strickly speaking, N runs from 0 to ∞. Since we are summing this numerically, we obviously need cut-off points. Because $L_N(\nu)$ varies more slowly than $p(N)$ as a function of N, we can determine the upper and lower cut-off points N_U, N_L by the distribution of $p(N)$. There are two cases: (*a*) $\bar{N} < 100$. We pick N_U and N_L to be the first values of N, above and below the mean, respectively, such that $p(N) < 0.05 \times$ MAX $p(N)$ and set:

$$\sum_{N=0}^{\infty} L_N(\nu)p(N) = \sum_{N=N_L}^{N_U} L_N(\nu)p(N). \tag{A1}$$

(*b*) $\bar{N} > 100$. This case is more complicated. First of all, to insure we have enough terms, we choose $N_U = \bar{N} + 3.2\sqrt{N}$, and $N_L = \bar{N} - 3.2\sqrt{N}$. This means that we will include all the values within 3.2 SD on both sides of the mean. We could use Eq. (A1) but this means we will be taking about $6.4\sqrt{N}$ terms, and this is not feasible when $\bar{N}$ is large. Instead we can treat $\Sigma_{N=0}^{\infty} L_N(\nu)p(N)$ as an integral. We can divide the $6.4\sqrt{N}$ interval into 48 subintervals, and evaluate $L_N(\nu)p(N)$ at the endpoints of these subintervals (49 points total). Then we apply Simpson's rule to evaluate the integral.

APPENDIX B

"Experimental" Value of ρ for a Pore Mechanism

The transport of K^+ ions across a dioleoyllecithin (DOL) black lipid membrane by valine gramicidin A at 25°C has been assumed to occur via a pore mechanism (Läuger, 1975; Läuger, 1973). Läuger has shown that, for a particular model of this mechanism, the tracer permeability coefficient is given by (Läuger, 1973):

$$P^* = \left\{\frac{N_p \upsilon}{1 + cK}\right\}\left\{\frac{k_0}{1 + \sum_{\nu=1}^{n} S_\nu}\right\}, \tag{B1}$$

where N_p is the number of pores per unit area of membrane, υ, is the volume of aqueous solution from which an ion can "jump" into a pore, c is the total ion concentration (tracer plus nontracer) in the aqueous phase, K and k_0 are the Langmuir equilibrium quotient and the first-order rate constant for the binding of an ion to a pore, respectively, (n + 1) is the number of activation barriers in the pore model, and S_ν is a ratio of products of first-order rate constants for the movement of an ion through the pore. For the DOL/gramicidin A/K^+ system at 25°C, Läuger gives υ as 100 Å^3, K as 4.3 M^{-1}, and n as 5 (Läuger, 1973). From the values of other appropriate rate constants given by Läuger (1973), k_0 and $\Sigma_{\nu=1}^{5} S_\nu$ can be calculated to be 1.9×10^9 s^{-1} and 2.3, respectively. Subsequent, more sophisticated, models for the valine gramicidin A pore (Stevens and Tsien, 1979; Eisenman et al., 1978; Levitt, 1978) are almost certainly more appropriate. However, the rate constants given here are "experimental" facts in the sense that Läuger's simple model was "fitted" to experimentally observed conductances.

For a typical NMR experiment, of the type described in this paper, on small vesicles (~100-Å radius) containing one pore each ($\bar{M} = 2$; $m = 2$ for the gramicidin A dimeric pore), the value of N_p would be 8.0×10^{-6} pore/Å^2. The value of c would be typically 10^{-2} M. Thus, we calculate that P^* would be 4.4×10^5 Å/sec for such an experiment. For the purpose of this calculation, let us use the approximation:

$$A\left\{\frac{P^*_{in}}{V_{out}} + \frac{P^*_{out}}{V_{in}}\right\} \simeq \left\{\frac{A}{V_{in}}\right\} P^*. \tag{B2}$$

(This is probably quite nearly true for small vesicles where $V_{out} \gg V_{in}$, if $P^*_{out} \sim P^*_{in}$.) Thus, combining Eq. B2 with Eq. 10, we have

$$\left\{\frac{A}{V_{in}}\right\} P^* = \beta_{eff}. \tag{B3}$$

The quantity (A/V_{in}) is a vesicle constant (the "claustrophobic ratio") with units of Å^{-1} here. It becomes smaller as the size of the vesicle increases. For example, for small, sonicated vesicles an average value for (A/V_{in}) of 0.59 Å^{-1} has been measured (Chrzeszczyk et al., 1977). Using 0.5 Å^{-1} we obtain a value for β_{eff} of 2.2×10^5 s^{-1}. For the first-order approximation of β_{eff} and for a vesicle with M mediators, we have

$$\beta_{eff} = \rho\gamma\left|\frac{M}{m}\right|. \tag{B4}$$

From Läuger's value of k_R, the rate constant for formation of the activated pore (2.4×10^{14} cm^2 mol^{-1} s^{-1}; Läuger, 1975), and the value of N_P given above, we can evaluate $\gamma|^M_m|$ to be 64 s^{-1} in our case. Thus, we obtain for ρ the value 3,500. Clearly, these are very efficient pulses.

In this case, we also know t_p, since it is equal to k_D^{-1}, where k_D is the first-order rate constant for deactivation of the pore. Läuger (1975) gives a value for k_D of 1.6 s^{-1} making t_p = 0.62 s. Therefore, β_0, given by ρ/t_p, is 5,500 s^{-1} for the gramicidin pulses.

APPENDIX C

"Experimental" Value of ρ for a Mobile Carrier Mechanism

The transport of K^+ across a phosphatidylinositol (PI) black lipid membrane by valinomycin at 25°C has been assumed to occur via a mobile (diffusive) carrier mechanism (Läuger, 1975, 1972; Stark et al., 1971). Läuger and Stark have shown that, for such a mechanism, the tracer permeability coefficient is given by (Läuger and Stark, 1970):

$$P^* = \frac{d}{2}\left\{\frac{c_0 K'}{1 + cK'}\right\}\left\{\frac{\gamma_{MS} k_{MS}}{1 + 2k_{MS}/k'_D}\right\}, \tag{C1}$$

where d is the thickness of the membrane, c_0 is the concentration of valinomycin in the aqueous phase, K' is the homogeneous equilibrium quotient for the binding of K^+ to valinomycin in water, c is the total ion concentration (tracer plus nontracer) in the aqueous phase (same as in Appendix B), γ_{MS} is the partition coefficient of the valinomycin/K^+ complex into the membrane from the aqueous phase, k_{MS} is the first-order rate constant for the diffusion of this complex across the membrane, and k_D' is the first-order rate constant for the dissociation of this complex at the membrane interface to deliver the metal ion to the aqueous phase. For the PI/valinomycin/K^+ system at 25°C, Stark et al. (1971) gives values for $K' \cdot \gamma_{MS} \cdot k_{MS}$ of 1.2×10^9 M^{-1} s^{-1}, k_{MS} of 2×10^4 s^{-1}, and k_D' of 5×10^4 s^{-1}. Since a value for c_0 of 10^{-7} M gives rise to 1.2×10^{12} valinomycin molecules/cm^2 (of membrane) (Läuger, 1972), a value for c_0 of 7×10^{-9} M would be appropriate for one valinomycin molecule per small vesicle (see Appendix B for the average surface area per small vesicle). Thus, taking $d/2$ to be 25 Å and a value for c of 10^{-2} M (see Appendix B), we obtain a value for P^* of 115 Å/s.

Again, using Eq. B3 and a value of 0.5 Å^{-1} for A/V_{in} (Appendix B), we obtain a value of 57 s^{-1} for β_{eff}. Since, in this case M = 1 (recall our value of c_0, above) and m = 1 (the conventional wisdom for valinomycin mediated transport), $|^M_m|$ = 1 and Eq. B4 tells us that $\rho\gamma$ = 57 s^{-1} here. To evaluate ρ, we must have a value for γ. If we define a mediating event to be one round trip of the carrier molecule whether or not it delivers any cation, then γ is essentially equal to the maximum turnover number, which for this mechanism is given by the expression $(k_{MS}^{-1} + k_S^{-1} + 2k_D'^{-1})^{-1}$ (Läuger, 1972), where k_S is the first-order rate constant for the diffusion of the empty carrier molecule across the membrane and, for this system, has a value of 2×10^4 s^{-1} (Stark et al., 1971). Thus we obtain a value of γ of 7×10^3 s^{-1}. This gives us a value for ρ of 8×10^{-3}. Thus, this "prototypical" mobile (diffusive) carrier-mediated transport would appear inefficient in the NMR experiment in terms of our model even though, as Läuger (1972) points out, a γ of 10^4 s^{-1} is quite efficient, in the frequency sense, compared to typical enzyme kinetics.

We would like to thank the National Science Foundation for grants PCM-7600193 and PCM-7807918 (to C. S. Springer) and the National Institute of General Medical Sciences for grant GM 22432 (to S. I. Chan) in support of this work.

Received for publication 29 August 1979 and in revised form 22 December 1980.

REFERENCES

Bergelson, L. D. 1977. Paramagnetic hydrophilic probes in NMR investigations of membrane systems. *Methods Membr. Biol.* 9:275.

Bergelson, L. D., L. I. Barsukov, N. I. Dubrovina, and V. F. Bystrov. 1970. Differentiation of the interior and exterior surfaces of phospholipid membranes by NMR spectroscopy. *Dokl. Akad. Nauk (SSSR).* 194:708.

Bergelson, L. D., and V. F. Bystrov. 1975. Use of shift and broadening reagents in the NMR investigation of membranes. *In* Biomembranes: Structure and Function. G. Gardos and I. Szasz, editors. American Elsevier 35:33.

Chen, S.-T. 1978. The antibiotic lasalocid A (X-537A): NMR studies employing paramagnetic lanthanide ions. Ph.D. Dissertation. State University of New York, Stony Brook, New York.

Chrzeszczyk, A. 1978. Charge, size, and structure of highly curved vesicles. Ph.D. Dissertation. State University of New York, Stony Brook, New York.

Chrzeszczyk, A., A. Wishnia, and C. S. Springer. 1977. The intrinsic structural asymmetry of highly curved phospholipid bilayer membranes. *Biochim. Biophys. Acta.* 470:161.

Chrzeszczyk, A., A. Wishnia, and C. S. Springer. 1976. Hyperfine induced splitting of free solute nuclear magnetic resonances in small phospholipid vesicle preparations. *ACS Symp. Ser.* 34:483.

Cushley, R. J., and B. J. Forrest. 1977. Structure and stability of vitamin E-lecithin and phytanic acid-lecithin bilayers studied by ^{13}C and ^{31}P nuclear magnetic resonance. *Can. J. Chem.* 55:220.

Degani, H. 1978. NMR kinetic studies of the ionophore X-537-A mediated transport of manganous ions across phospholipid bilayers. *Biochim. Biophys. Acta.* 509:364.

Degani, H., and G. Elgavish. 1978. Ionic permeabilities of membranes. ^{23}Na and ^{7}Li NMR studies of ion transport across the membrane of phosphatidylcholine vesicles. *FEBS (Fed. Eur. Biochem. Soc.) Lett.* 90:357.

Degani, H., and R. E. Lenkinski. 1980. Ionophoric properties of angiotensin II peptides. Nuclear magnetic resonance kinetic studies of the hormone mediated transport of manganese ions across phosphatidylcholine bilayers. *Biochemistry.* 19:3430.

DeKruijff, B., and R. A. Demel. 1974. Polyene antibiotic-sterol interactions in membranes of *Acholesplasma laidlawii* cells and lecithin liposomes. III. Molecular structure of the polyene antibiotic-cholesterol complexes. *Biochim. Biophys. Acta.* 339:57.

Eisenman, G., J. Sandblom, and E. Neher. 1978. Interactions in cation permeation through the gramicidin channel. *Biophys. J.* 22:307.

Ermishkin, L. N., Kh. M. Kasumov, and V. M. Potzeluyer. 1976. Single ionic channels induced in lipid bilayers by polyene antibiotics amphotericin B and nystatine. *Nature (Lond.)* 262:698.

Fernandez, M. S., H. Celis, and M. Montal. 1973. Proton magnetic resonance detection of ionophore mediated transport of praseodymium ions across phospholipid membranes. *Biochim. Biophys. Acta.* 323:600.

Finkelstein, A., and R. Holz. 1973. Aqueous pores created in thin lipid membranes by the polyene antibiotics nystatin and amphotericin B. *In* Membranes, A Series of Advances. Lipid Bilayers and Antibiotics. G. Eisenman, editor. Marcel Dekker. New York. p. 377.

Gent, M. P. N., and J. H. Prestegard. 1976. Interaction of polyene antibiotics with lipid bilayer vesicles containing cholesterol. *Biochim. Biophys. Acta.* 426:17.

Gerritsen, W. J., E. J. J. Van Zoelen, A. J. Verkleij, B. DeKruijff, and L. L. M. Van Deenen. 1979. A ^{13}C NMR method for determination of the transbilayer distribution of phosphatidylcholine in large, unilamellar, protein-free and protein-containing vesicles. *Biochim. Biophys. Acta.* 551:248.

Heer, C. V. 1972. Statistical Mechanics, Kinetic Theory, and Stochastic Processes. Academic Press, Inc., New York. pp. 99 and 420.

Hladky, S. B., L. G. M. Gordon, and D. A. Haydon. 1974. Molecular mechanisms of ion transport in lipid membranes. *Ann. Rev. Phys. Chem.* 25:11.

Hunt, G. R. A. 1975. Kinetics of ionophore-mediated transport of Pr^{+3} ions through phospholipid membranes using ^{1}H NMR spectroscopy. *FEBS (Fed. Eur. Biochem. Soc.) Lett.* 58:194.

Hunt, G. R. A. 1980. A comparison of Triton X-100 and the bile salt taurocholate as micellar ionophores or fusogens in phospholipid vesicular membranes. *FEBS (Fed. Eur. Biochem. Soc.) Lett.* 119:132.

Hunt, G. R. A., and K. Jawaharlal. 1980. A ^{1}H NMR investigation of the mechanism for the ionophore activity of the bile salts in phospholipid vesicular membranes and the effect of cholesterol. *Biochim. Biophys. Acta.* 601:678.

Hunt, G. R. A., and L. R. H. Tipping. 1978. A ^{1}H NMR study of the effects of metal ions, cholesterol, and *n*-alkanes on phase transitions in the inner and outer monolayers of phospholipid vesicular membranes. *Biochim. Biophys. Acta.* 507:242.

Hunt, G. R. A., L. R. H. Tipping, and M. R. Belmont. 1978. Rate-determining processes in the transport of Pr^{+3} ions by the ionophore A-23187 across phospholipid vesicular membranes. A ^{1}H-NMR and theoretical study. *Biophys. Chem.* 8:341.

Hutton, W. C., P. L. Yeagle, and R. B. Martin. 1977. The interaction of lanthanide and calcium salts with phospholipid bilayer vesicles: the validity of the nuclear magnetic resonance method for determination of vesicle bilayer phospholipid surface ratios. *Chem. Phys. Lipids.* 19:255.

Korenbrot, J. I. 1977. Ion transport in membranes: incorporation of biological ion-transporting proteins in model membrane systems. *Ann. Rev. Physiol.* 39:19.

Lau, A. L. Y., and S. I. Chan. 1976. Voltage-induced formation of alamethicin pores in lecithin bilayer vesicles. *Biochemistry.* 15:2551.

Lau, A. L. Y., and S. I. Chan. 1975. Alamethicin-mediated fusion of lecithin vesicles. *Proc. Natl. Acad. Sci. U.S.A.* 72:2170.

Läuger, P. 1975. Ion transport through artificial lipid membranes. *Adv. Chem. Phys.* 29:309.

Läuger, P. 1973. Ion transport through pores: a rate-theory analysis. *Biochim. Biophys. Acta.* 311:423.

Läuger, P. 1972. Carrier mediated ion transport. *Science (Wash. D. C.)* 178:24.

Läuger, P., and G. Stark, 1970. Kinetics of carrier-mediated ion transport across lipid bilayer membranes. *Biochim. Biophys. Acta.* 211:458.

Lawaczeck, R., D. Blackman, and M. Kainosho. 1977. Ion permeation across the bilayer of annealed phosphatidylcholine vesicles at elevated temperatures. Concentration dependence and the micelle-bilayer dynamic equilibrium. *Biochim. Biophys. Acta.* 468:411.

Lawaczeck, R., M. Kainosho, and S. I. Chan. 1976. The formation and annealing of structural defects in lipid bilayer vesicles. *Biochim. Biophys. Acta.* 443:313.

Lee, Y., and S. I. Chan. 1977. The effect of lysolecithin on the structure and permeability of lecithin bilayer vesicles. *Biochemistry.* 16:1303.

Levitt, D. G. 1978. Electrostatic calculations for an ion channel. II. Kinetic behavior of the gramicidin A channel. *Biophys. J.* 22:221.

McLaughlin, S., and M. Eisenberg. 1975. Antibiotics and membrane biology. *Ann. Rev. Biophys. Bioeng.* 4:335.

Michaelson, D. M., A. F. Horwitz, and M. P. Klein. 1973. Transbilayer asymmetry and surface homogeneity of mixed phospholipids in cosonicated vesicles. *Biochemistry.* 12:2637.

Montal, M. 1976. Experimental membranes and mechanisms of bioenergy transductions. *Ann. Rev. Biophys. Bioeng.* 5:119.

Neher, E., and C. F. Stevens. 1977. Conductance fluctuations and ionic pores in membranes. *Ann. Rev. Biophys. Bioeng.* 6:345.

O'Brien, D. F., N. Zumbulyadis, F. M. Michaels, and R. A. Ott. 1977. Light-regulated permeability of rhodopsin: egg phosphatidylcholine recombinant membranes. *Proc. Natl. Acad. Sci. U.S.A.* 74:5222.

Pierce, H. D., A. M. Unrau, and A. C. Oehlschlager. 1978. Investigation of polyene macrolide antibiotic-induced permeability changes in vesicles by ^{31}P nuclear magnetic resonance. *Can J. Biochim.* 56:801.

Scott, H. L., and S.-L. Cherng. 1978. Monte Carlo studies of phospholipid lamellae: effects of confinement by head groups, proteins, cholesterol, and bilayer curvature on order parameters. *Biochem. Biophys. Acta.* 510:209.

Shamoo, A. E., and D. A. Goldstein. 1977. Isolation of ionophores from ion transport systems and their role in energy transduction. *Biochim. Biophys. Acta.* 472:13.

Sheetz, M. P., and S. I. Chan. 1972. Effect of sonication on the structure of lecithin bilayers. *Biochemistry.* 11:4573.

Sjodin, R. A. 1971. Ion transport across excitable cell membranes. *In* Biophysics and Physiology of Excitable Membranes. W. J. Adelman, editor. Van Nostrand Reinhold, New York. Chap. 3, p. 96.

Stark, G., B. Ketterer, R. Benz, and P. Läuger. 1971. The rate constants of valinomycin-mediated ion transport through thin lipid membranes. *Biophys. J.* 11:981.

Stevens, C. F., and R. W. Tsien. 1979. Ion permeation through membrane channels. *In* Membrane Transport Processes. Vol. 3. Raven Press, New York.

Szoka, F., and D. Paphadjoupoulos. 1980. Comparative properties and methods of preparation of lipid vesicles (liposomes). *Ann. Rev. Biophys. Bioeng.* 9:467.

Van Hoogevest, P., and B. DeKruijff. 1978. Effect of amphotericin B on cholesterol-containing liposomes of egg phosphatidyl and didocosenoyl phosphatidylcholine *Biochim. Biophys. Acta.* 511:397.

Van Kampen, N. G. 1976. Stochastic differential equations. *Phys. Lett.* C 24:171.

Waldbillig, R. C., and G. Szabo. 1979. Planar bilayer membranes from pure lipids. *Biochim. Biophys. Acta.* 557:295.

White, S. H. 1977. Studies of the physical chemistry of planar bilayer membranes using high precision measurements of specific capacitance. *Ann. N. Y. Acad. Sci.* 303:243.

White, S. H. 1978. Formation of "solvent-free" black lipid bilayer membranes from glyceryl monooleate dispersed in squalene. *Biophys. J.* 23:337.